Wavelength Dependence of Excimer Laser Photolysis of $Cr(CO)_6$ in the Gas Phase. A Study of the Infrared Spectroscopy and Reactions of the $Cr(CO)_x$ (x = 5, 4, 3, 2) Fragments

T. A. Seder, Stephen P. Church,† and Eric Weitz*

Contribution from the Department of Chemistry, Northwestern University, Evanston, Illinois 60201. *Received February 14, 1986*

Abstract: The transient infrared absorption spectra of the coordinatively unsaturated $Cr(CO)_x$ species (x = 5, 4, 3, and 2) that are generated via excimer laser photolysis of gas-phase $Cr(CO)_6$ are presented and discussed. The photofragments produced upon 193-, 248-, and 351-nm photolysis are identified. The results indicate that the gas-phase structures of the $Cr(CO)_x$ species are the same as those observed in condensed-phase experiments. It is postulated that $Cr(CO)_5$ adopts a C_{4v} structure, $Cr(CO)_4$ adopts a C_{2v} structure, and $Cr(CO)_3$ adopts a C_{3v} structure. The coordinatively unsaturated species are, in general, observed to be produced with a significant amount of internal excitation. The rate constants for the reaction of $Cr(CO)_5$, $Cr(CO)_4$, and $Cr(CO)_3$ with CO were measured and found to be 1.5×10^{13}, 2.4×10^{13}, and 1.8×10^{13} cm^3 mol^{-1} s^{-1}, respectively.

I. Introduction

The photochemistry of organometallic complexes is an area of vigorous research.[1] Of the simple transition-metal carbonyls, $Cr(CO)_6$ is probably the most extensively studied.[2] The primary photoprocess in condensed phases is ejection of one CO ligand,[1-9]

$$Cr(CO)_6 \xrightarrow{h\nu} Cr(CO)_5 + CO \qquad (1)$$

Detailed IR[3] and UV–vis[4] spectroscopic studies have shown that, in low-temperature matrices (20 K), $Cr(CO)_5$ has a square-pyramidal (C_{4v}) geometry with a matrix atom occupying the sixth (vacant) site. Lower fragments $Cr(CO)_x$ (x = 4, 3, 2) are generated through sequential single-photon absorption by the respective $Cr(CO)_{x+1}$ species.[5] Analysis of the structures of these fragments led to some surprising results, e.g., $Cr(CO)_4$ had a low-symmetry C_{2v} geometry.[5] Because of this low symmetry, there remained a question as to whether solid-state effects perturbed the molecules from their "ideal" gas-phase structures.

The transient $Cr(CO)_5$ species, weakly interacting with the solvent, has been detected via flash photolysis of room temperature solutions of $Cr(CO)_6$.[6-9] Pioneering experiments of Kelly, Koerner von Gustorf, and co-workers using UV–vis detection provided rate constants for reaction of $Cr(CO)_5{\cdot}C_6H_{12}$ with CO and other ligands.[6] Further studies in noncoordinating perfluoro solvents revealed the extraordinarily high reactivity of $Cr(CO)_5$.[7] Indeed, Welch et al.[8] have shown that $Cr(CO)_5$ coordinates to the solvent medium within 25 ps of photoexcitation of $Cr(CO)_6$. More recent experiments with IR detection indicated that in room temperature solution $Cr(CO)_5$ adopts a C_{4v} geometry.[9]

The gas-phase photochemistry and photophysics of $Cr(CO)_6$ are less well studied. Studies by Breckenridge et al.,[10] employing a frequency tripled Nd/Yag laser (355 nm) as a photolysis source, provided evidence for gas-phase $Cr(CO)_5$ as well as polynuclear chromium species through their transient visible absorptions. A chemical trapping study of Tumas et al.[11] provided the first evidence that the gas-phase photochemistry of $Cr(CO)_6$ is different than that in solution. Their results suggested that $Cr(CO)_x$ (x = 5, 4, 3, 2) species were produced upon 248-nm (KrF laser) single-photon excitation of $Cr(CO)_6$. By analogy to similar experiments with $Fe(CO)_5$,[12] it is apparent that increasing the energy of the input photon results in a higher degree of photofragmentation. Coordinatively unsaturated species were, however, not directly observed by this route.

The studies of Ouderkirk et al.[13] provided direct spectroscopic evidence for coordinatively unsaturated metal carbonyls in the gas phase. $Fe(CO)_x$ species (x = 2, 3, 4) were generated from excimer laser photolysis of $Fe(CO)_5$ and probed via their intense CO stretching vibrations with a line-tunable CO laser. The results gave photophysical, kinetic, and structural information and confirmed that more highly coordinatively unsaturated species were formed in greater yield with a higher energy input photon. A recent gas-phase study of $Cr(CO)_6$ with a XeF laser (351 nm)[14] showed that the dominant photoproduct at this wavelength was $Cr(CO)_5$. As found in the matrix,[3] in solution,[9] and as predicted by molecular orbital calculations,[15] this gas-phase species adopts a square-pyramidal structure. A related study by Fletcher and Rosenfeld[16] showed that with a photolysis wavelength of 248 nm the major product was $Cr(CO)_4$. Though their work provided some kinetic data, it gave no detailed spectral information.

† Present address: Max Planck Institut fur Strahlenchemie, D-4330 Mulheim a.d. Ruhr, West Germany.

(1) Geoffroy, G. L.; Wrighton, M. S. *Organometallic Photochemistry*; Academic Press: New York, 1979.
(2) Turner, J. J.; Poliakoff, M. *ACS Symp. Ser.* **1983**, *No. 211*, 35.
(3) Perutz, R. N.; Turner, J. *J. Inorg. Chem.* **1975**, *14*, 262.
(4) Perutz, R. N.; Turner, J. J. *J. Am. Chem. Soc.* **1975**, *97*, 4791.
(5) Perutz, R. N.; Turner, J. J. *J. Am. Chem. Soc.* **1975**, *97*, 4800.
(6) Kelly, J. M.; Hermann, H.; Koerner von Gustorf, E. *J. Chem. Soc., Chem. Commun.* **1973**, 105. Kelly, J. M.; Bent, D. V.; Hermann, H.; Schulte-Frohlinde, D.; Koerner von Gustorf, E. *J. Organomet. Chem.* **1974**, *69*, 259.
(7) Bonneau, R.; Kelly, J. M. *J. Am. Chem. Soc.* **1980**, *102*, 1220. Kelly, J. M.; Long, C.; Bonneau, R. *J. Phys. Chem.* **1983**, *87*, 3344.
(8) Welch, J. A.; Peters, K. S.; Vaida, V. *J. Phys. Chem.* **1982**, *86*, 1941.
(9) Church, S. P.; Grevels, F.-W.; Hermann, H.; Schaffner, K. *Inorg. Chem.* **1985**, *24*, 418.
(10) Breckenridge, W. H.; Sinai, N. *J. Phys. Chem.* **1981**, *85*, 3557. Breckenridge, W. H.; Stewart, G. M. *J. Am. Chem. Soc.* **1986**, *108*, 364.
(11) Tumas, W.; Gitlin, B.; Rosan, A. M.; Yardley, J. T. *J. Am. Chem. Soc.* **1982**, *104*, 55.
(12) Yardley, J. T.; Gitlin, B.; Nathanson, G.; Rosan, A. M. *J. Chem. Phys.* **1981**, *74*, 361, 370.
(13) Ouderkirk, A. J.; Wermer, P.; Schultz, N. L.; Weitz, E. *J. Am. Chem. Soc.* **1983**, *105*, 3354. Ouderkirk, A. J.; Weitz, E. *J. Chem. Phys.* **1983**, *79*, 1089. Ouderkirk, A. J.; Seder, T. A.; Weitz, E. *SPIE Symp. Appl. Lasers Ind. Chem.* **1984**, *458*, 148. Seder, T. A.; Ouderkirk, A. J.; Weitz, E., to be published.
(14) Seder, T. A.; Church, S. P.; Ouderkirk, A. J.; Weitz, E. *J. Am. Chem. Soc.* **1985**, *107*, 1432.
(15) Burdett, J. K. *J. Chem. Soc., Faraday Trans. 2* **1974**, *70*, 1599. Elian, M.; Hoffmann, R. *Inorg. Chem.* **1975**, *14*, 1058.
(16) (a) Fletcher, T. R.; Rosenfeld, R. N. *J. Am. Chem. Soc.* **1985**, *107*, 2203. (b) Fletcher, T. R.; Rosenfeld, R. N. *J. Am. Chem. Soc.* **1986**, *108*, 1686.
(17) Lewis, K. E.; Golden, D. M.; Smith, G. P. *J. Am. Chem. Soc.* **1984**, *106*, 3905.
(18) Graham, M. A.; Poliakoff, M.; Turner, J. J. *J. Chem. Soc. A.* **1971**, 2939.
(19) Turner, J. J.; Burdett, J. K.; Perutz, R. N.; Poliakoff, M. *Pure Appl. Chem.* **1977**, *49*, 271.
(20) Demuynck, J.; Kochanski, E.; Veillard, A. *J. Am. Chem. Soc.* **1979**, *101*, 3467.

0002-7863/86/1508-4721$01.50/0

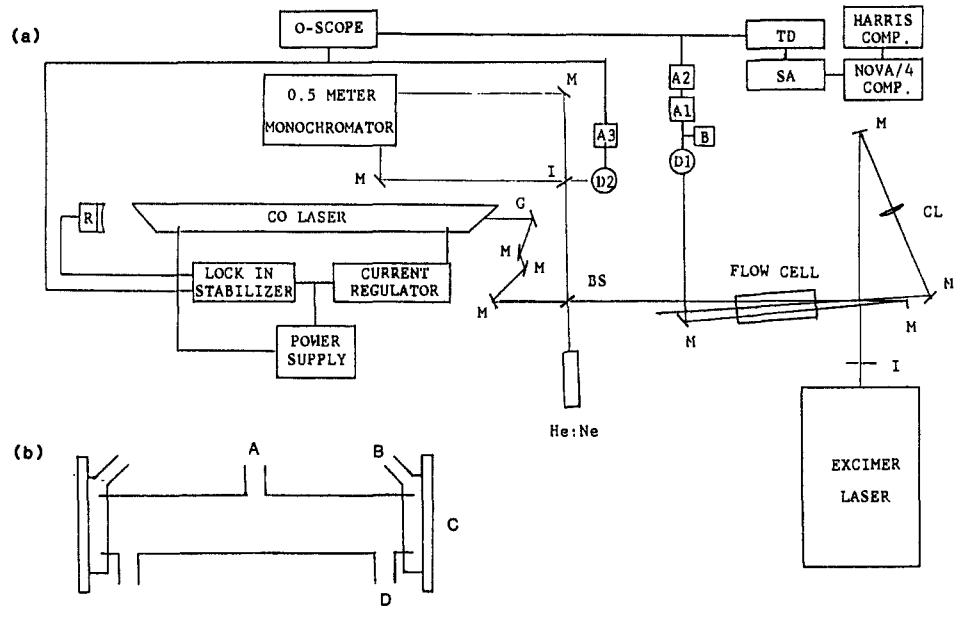

Figure 1. Schematic diagram of transient absorption apparatus. Symbols for a: A, amplifier; B, reverse bias for InSb detector; BS, beam splitter; CL, cylindrical line; D1, InSb detector; D2, AuGe detector; G, grating; I, tris; M, mirror; SA, signal averager; TD, transient digitizer. Symbols for the photolysis cell (b): A, sample gases in; B, window purge in; C, CaF_2 window; D, exhaust.

The aim of our present study is to systematically investigate the gas-phase photochemistry of $Cr(CO)_6$ at various photolysis wavelengths (351, 248, and 193 nm) and to analyze the structures and reactions of the resulting metal carbonyl fragments. We have at our disposal a means of observing unusual $Cr(CO)_x$ species (x = 5, 4, 3, 2) free from solid-state or solvent effects.

II. Experimental Section

The apparatus used for all measurements reported here is diagrammed schematically in Figure 1a. The output from the excimer laser (Questek 2000), operating on either XeF, KrF, or ArF, makes a single pass through the flow cell after passing through the BaF_2 cylindrical lens. Confirmation that the lens spatially homogenizes the UV pulse was obtained by visually examining the uniformity of the emission resulting when the pulse was intercepted with a fluorescent pad. The optical alignment was such that the UV pulse fills the entire volume of the flow cell. This procedure was necessary to avoid spurious signals resulting from both temperature and photoproduct inhomogeneities. The glass cell has a radius of 0.75 cm and an active length of 10 cm. The CaF_2 windows of the cell were protected from photofragments by a curtain of rare gas which flowed over the windows and out the exhaust ports without mixing with sample gases (Figure 1b). Photofragments and their reaction products were observed to be deposited only in the region between the two exhaust ports.

Sample gases enter at the center of the cell and exit through the exhaust ports. Before entering the cell each gas was first passed through a computer-controlled flow controller (Tylan), a gas-mixing manifold, and finally a 12-in. mixing tube which was packed with glass beads. A continuous flow of gas-phase $Cr(CO)_6$ was effected by directing a stream of Ar through a narrow, 30-in., temperature-jacketed glass column which was packed with glass beads and solid $Cr(CO)_6$. The partial pressure of $Cr(CO)_6$ in the flow could be controlled via both the temperature of and flow rate through the column. As determined by normal infrared spectroscopy, the conditions for all experiments reported here were such that $Cr(CO)_6$ was sublimed at a rate necessary to deliver a partial pressure of approximately 30 mTorr to the cell. $Cr(CO)_6$ was obtained from Alfa Products (98% purity) and was sublimed in situ. Ar (99.99+% purity) and CO (99.99+% purity) were obtained from Matheson and used without prior purification.

The transient species that were produced by UV photolysis of $Cr(CO)_6$ were monitored via the output of a home-built, liquid nitrogen cooled, line tunable carbon monoxide laser. The continuous wave infrared beam, after making a double pass through the flow cell, was dispersed to fill the entire area of the element of an indium antimonide detector. For wavelength determination a portion of the IR beam was split and passed through a 0.5-m monochromator. The monochromator was equipped with a 10-μm grating and was calibrated for use in second order by comparison with the position of various orders of a HeNe laser line.

To obtain maximum linearity and detectivity the photovoltaic indium antimonide detector (1 mm × 1 mm in an SBRC Model 40742 side-looking dewar) was equipped with a variable back biasing circuit which allows operation at the origin of the i–v curve of the detector. The output of this detector was amplified (×100, Perry 070/40), fed through a unity gain buffer amplifier (Perry), and ultimately digitized by a Biomation 8100 waveform recorder. Typically, 64 waveforms were averaged via simple addition by a Nicolet 1170 signal averager. The resulting signals were stored on a Nova/4 minicomputer which is in communication with a Harris super-minicomputer. The Harris Computer was used for signal analysis. The measured response time of the detection system was 35 ns.

Time resolved transient infrared spectra were obtained as follows. The In:Sb detector was nulled for a probe beam intensity of ~5 mW at a particular frequency. Following acquisition of the waveform, the probe frequency was changed and the intensity was matched to that of the previous frequency via adjustment of an aperture positioned in the cavity of the CO laser. A second waveform was then recorded. This procedure was repeated for numerous probe frequencies within the carbonyl stretch region. From the series of resulting waveforms, a transient infrared spectrum was computer constructed by joining together the amplitude of each waveform at a particular time.

Kinetic information was obtained by probing the relevant regions of the spectrum while varying the concentration of added CO. Resulting waveforms were analyzed as multiple exponentials by an iterative Guggenheim procedure[22] and/or via a Provencher procedure.[23]

III. Results and Discussion

The infrared stretching absorptions of $Cr(CO)_x$, where x = 5–2, generally occur at lower frequency than those of $Cr(CO)_{x+1}$ due to the increase in metal–ligand back-bonding. The frequency and intensity of the infrared absorption bands observed in these gas-phase experiments are strongly dependent upon photolysis wavelength. In general, a greater predominance of lower frequency bands is observed as the photolysis energy increases, indicating that the product distribution shifts toward the more highly unsaturated fragments. The fragments that comprise the distribution resulting upon XeF (351, 353 nm), KrF (248 nm), and ArF (193 nm) laser photolysis will be identified and discussed in the order of increasing photolysis energy. Fragments are identified, and their gas-phase structures are postulated on the basis of the position and kinetic behavior of their absorption bands.

XeF Laser Photolysis. The infrared spectrum 0.5 μs following XeF laser photolysis of $Cr(CO)_6$ is shown in Figure 2a. The XeF

(21) Burdett, J. K.; Graham, M. A.; Perutz, R. N.; Poliakoff, M.; Rest, A. J.; Turner, J. J.; Turner, R. F. *J. Am. Chem. Soc.* **1975**, *97*, 4085.

(22) Ouderkirk, A. J. Ph.D. Thesis, Northwestern University, 1983.

(23) Provencher, S. W. *Biophys. J.* **1976**, *16*, 27. Provencher, S. W. *J. Chem. Phys.* **1976**, *64*, 2772.

Table I. Infrared Absorptions of Matrix-Isolated and Gas-Phase $Cr(CO)_x$

	freq (cm^{-1}) Ar matrix	gas phase[a]	assign	symmetry	ref
$Cr(CO)_5$	2093.4		A_1	C_{4v}	18
	1965.4	1980	E		
	1936.1	1948	A_1		
$Cr(CO)_4$			A_1	C_{2v}	21
	1938	1957	B_1		
	1932		A_1		
	1891	1920	B_2		
$Cr(CO)_3$	1867	1880	E	C_{3v}	5
$Cr(CO)_2$	1903[b]	1914	?	?	5

[a] Approximate values from this work. [b] CH_4 matrix.

laser inputs 82 kcal/mol. Since the $Cr(CO)_5$–CO bond energy is approximately 37 kcal/mol and the $Cr(CO)_4$–CO bond energy is estimated to be 40 kcal/mol,[17] 82 kcal/mol is in principal sufficient to remove two CO ligands. Thus it is expected that the positive absorptions in Figure 2a belong to both $Cr(CO)_5$ and $Cr(CO)_4$. The negative going peak represents photolytic depletion and is clearly the T_{1u} mode of $Cr(CO)_6$. In an Ar matrix, bands observed at 1965.4 and 1936.1 cm^{-1} have been attributed to absorption by C_{4v} $Cr(CO)_5$ (Table I). Since the absorption frequency of Ar matrix isolated species are in general shifted to lower frequency relative to that of the gas-phase species by 10–20 cm^{-1}, we assign the bands centered at 1980 and 1948 cm^{-1} (denoted by arrows in Figure 2a) as the E and one of the A_1 modes of C_{4v} $Cr(CO)_5$. (The remaining infrared active (A_1) CO stretching mode is expected to be weak and lies outside of the range of our probe laser.[18]) Although the band intensities can only be roughly compared due to the relatively low resolution of this spectrum, note that the intensity ratio of the E to the observed A_1 mode is roughly 4 to 1 and that of the T_{1u} mode of $Cr(CO)_6$ to the E mode of $Cr(CO)_5$ is ~3 to 2. These ratios are as expected on the basis of simple intensity arguments.[24]

Convincing kinetic evidence supporting assignment of the 1980- and 1948-cm^{-1} bands to $Cr(CO)_5$ can be obtained via observing the temporal behavior of these bands, as well as that of the parent, as a function of added CO. The dominant route for parent regeneration is anticipated to be via reaction of $Cr(CO)_5$ with CO. Complex kinetic schemes involving parent regeneration via reaction of polynuclear species with CO can easily be discounted on the basis of the expected time scale for these events at the concentration of polynuclear species present. Further, that the growth of new bands in the time-resolved spectrum is not observed, as would be expected if the distribution of fragments generated upon XeF laser photolysis contained significant amounts of chromium carbonyl fragments that are more highly unsaturated than $Cr(CO)_5$, indicates that the $Cr(CO)_5$ fragment dominates the distribution. The dominant process upon addition of CO is

$$Cr(CO)_5 + CO \xrightarrow{k_{56}} Cr(CO)_6 \qquad (2)$$

As discussed in detail later in the text, the $Cr(CO)_6$ species, which is initially produced with internal excitation, is rapidly stabilized. The rate-limiting step in forming $Cr(CO)_6$ is thus reaction 2. As is expected on the basis of our assignments, the 1980- and 1948-cm^{-1} bands return to the base line at the same rate as does the parent band over a range of added CO pressures of 0.5–5 Torr. The slope of the line obtained when the observed rate for process 2 is plotted against added CO pressure gives a second-order rate constant of $(1.5 \pm 0.3) \times 10^{13}$ cm^3 mol^{-1} s^{-1} for the recombination reaction. (These error brackets for this and subsequently reported numbers represent 95% confidence limits.) This rate constant is only approximately an order of magnitude slower than a gas kinetic rate constant and is consistent with the observed highly reactive behavior of solution-phase $Cr(CO)_5$.[6-9]

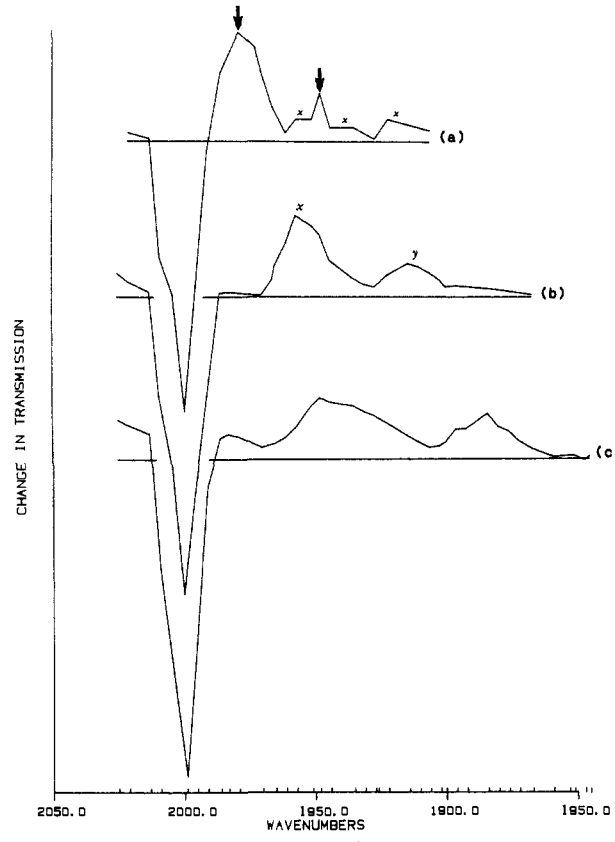

Figure 2. Dependence of the transient infrared absorption spectrum upon photolysis wavelength. The depicted spectra were constructed from transient absorptions observed 0.5 μs following (a) 351 nm (XeF), (b) 248 nm (KrF), and (c) 193 nm (ArF) photolysis of gas-phase $Cr(CO)_6$. See text for meaning of symbols and assignments of the absorption bands.

The position of the visible absorption of matrix-isolated $Cr(CO)_5$ is known to be strongly dependent upon the nature of the matrix material, shifting to longer wavelengths as the ionization potential of the matrix material increases. This matrix shift has been shown to be due to a stereospecific interaction between the a_1 orbital of $Cr(CO)_5$ and the matrix material, resulting in a change in the $e \rightarrow a_1$ transition energy.[19] The visible absorption of Ar-matrix-isolated $Cr(CO)_5$ is known to be so shifted.[19] It has also been reported that the $Cr(CO)_5\cdots Ar$ species was observed via conventional flash photolysis of gas-phase $Cr(CO)_6$ in the presence of Ar.[10] Since our measurements were performed in the presence of an Ar buffer, this implies that the rate constant reported above could be for the reaction

$$Cr(CO)_5\cdots Ar + CO \rightarrow Cr(CO)_6 + Ar$$

Although Viellard et al. report that (at the level of their SCF calculations) the Cr···Ar interaction is repulsive, it is possible that more refined calculations will show the Cr···Ar interaction to be, in fact, weakly attractive.[20] Thus complexation with rare gas in the gas phase is still a *potential* concern. To dispell this concern, we note that the rate constants measured both in the presence and in the absence of added buffer were the same, within experimental error. We thus do not believe the presence of the buffer introduces added complexity into the reaction kinetics. This is compatible with expectations based on the equilibrium constant for a weakly attractive gas-phase complex.

We have previously noted that the rate constant for the reaction of $Cr(CO)_5$ with CO is more than two orders of magnitude larger than the corresponding rate constant for the reaction of $Fe(CO)_4$ with CO.[14] We attributed this difference, in part, to spin conservation, noting that the ground states of $Fe(CO)_5$, $Cr(CO)_6$, and $Cr(CO)_5$ are singlets, whereas $Fe(CO)_4$ has a triplet ground state. We also indicated that steric constraints may be partly responsible for the differences in the observed recombination rates.[13] It is, however, unlikely that a major factor in the difference

(24) Braterman, P. S. *Metal Carbonyl Spectra*; Academic Press: London, 1975.
(25) Whetten, R. L.; Fu, K.-J.; Grant, E. R. *J. Chem. Phys.* **1983**, *79*, 4899.

in $Fe(CO)_4$ vs. $Cr(CO)_5$ rate constants for reaction with CO is due to steric effects, since the geometric transformation of C_{3v} $Fe(CO)_3$ into C_{2v} $Fe(CO)_4$ is not drastically different than that occurring when D_{3h} $Fe(CO)_5$ is formed through reaction of C_{2v} $Fe(CO)_4$ with CO.

The other positive absorptions in Figure 2a (labeled with x's) can be identified as the B_2, A_1, and B_1 vibrational modes of C_{2v} $Cr(CO)_4$ via correlation with matrix data (Table I). Due to the rather broad absorptions exhibited by gas-phase metal carbonyls, the B_1 and A_1 modes of $Cr(CO)_4$ are expected to be overlapped with one another as well as with the A_1 mode of $Cr(CO)_5$. On the basis of its observed position in an Ar matrix, the frequency of the B_2 mode is expected to be $\sim$1920 cm^{-1} in the gas phase. Note the weak absorption at $\sim$1920 cm^{-1} in Figure 2a. Due to the relatively low intensity of the bands assigned to $Cr(CO)_4$ produced via XeF photolysis of $Cr(CO)_5$, kinetic evidence supporting this assignment will be deferred until the fragments generated upon 248-nm photolysis are discussed.

The observation that $Cr(CO)_4$ is not formed in significant amounts upon XeF laser photolysis implies that $Cr(CO)_5$ must be born with significant internal energy. Of the 82 kcal/mol input by the XeF laser, 37 kcal/mol is consumed in $Cr(CO)_5$ formation.[17] The remaining 45 kcal/mol is partitioned between the translational and internal energies of the two fragments. The excess internal energy manifests itself via a shift of the spectral features of $Cr(CO)_5$ in the time resolved transient absorption spectrum shown in Figure 3b to higher energy. This figure displays the transient spectrum at successive $\sim$0.08-μs intervals following photolysis. The prominent shift to higher energy of the E mode of $Cr(CO)_5$ (1980 cm^{-1}) is indicative of collisional relaxation of the vibrational–rotational excitation in the nascent $Cr(CO)_5$. Also, note that the absence of an absorption in the region which would correspond to the $CO(v = 2) \rightarrow CO(v = 3)$ transition ($\sim$2020 cm^{-1}) signifies that only small amounts of $CO(v = 2)$ are generated. Though detailed measurements of the vibrational-state distribution of the photoejected CO have not as yet been made, the above result implies that direct absorption or emission experiments would reveal the vibrational-state distribution to be strongly dominated by CO in $v = 0, 1$.

Some evidence for the existence of polynuclear-forming reactions is displayed in the time-resolved spectrum of Figure 3a, which is analogous to that of Figure 3b except that the individual traces are separated by $\sim$0.3 μs. This spectrum illustrates that, while the bands of $Cr(CO)_5$ and $Cr(CO)_4$ have nearly returned to the base line, parent recovery is incomplete. Note the distortion of the T_{1u} band of $Cr(CO)_6$ as it returns to the base line. Though it is not conveniently shown for the time scale of the traces in Figure 3a, $Cr(CO)_6$ is further depleted on a time scale well beyond that expected if photolysis were the only mechanism responsible for $Cr(CO)_6$ depletion. These observations, as well as the fact that two long-lived absorptions at $\sim$1999 and $\sim$1991 cm^{-1} (denoted by arrows in Figure 3a) are observed, indicate the presence of reactions of the type

$$Cr(CO)_5 + Cr(CO)_6 \rightarrow Cr_2(CO)_{11} \quad (3)$$

or

$$Cr(CO)_4 + Cr(CO)_6 \rightarrow Cr_2(CO)_{10} \quad (4)$$

Reaction 3 has been observed in a perfluoromethylcyclohexane solvent by nanosecond flash techniques with visible detection.[7] The visible absorption of $Cr_2(CO)_{11}$ has also been observed following 355-nm photolysis of gas-phase $Cr(CO)_6$.[10] Reaction 4 has been reported by time-resolved infrared studies in the gas phase.[16] For XeF photolysis, we believe the reaction of $Cr(CO)_5$ with parent is the most important process since $Cr(CO)_5$ is the most abundant fragment, and a long-lived infrared absorption at 1980 cm^{-1}, which has previously been attributed to $Cr_2(CO)_{10}$,[16] is not observed. Thus we tentatively assign the absorptions at 1999 and 1991 cm^{-1} to $Cr_2(CO)_{11}$. Unfortunately, no reliable infrared data for $Cr_2(CO)_{11}$ in condensed phases are available for comparison purposes.

The appearance of the absorption bands attributed to $Cr_2(CO)_{11}$ in the time-resolved spectrum (Figure 3a) implies that reaction

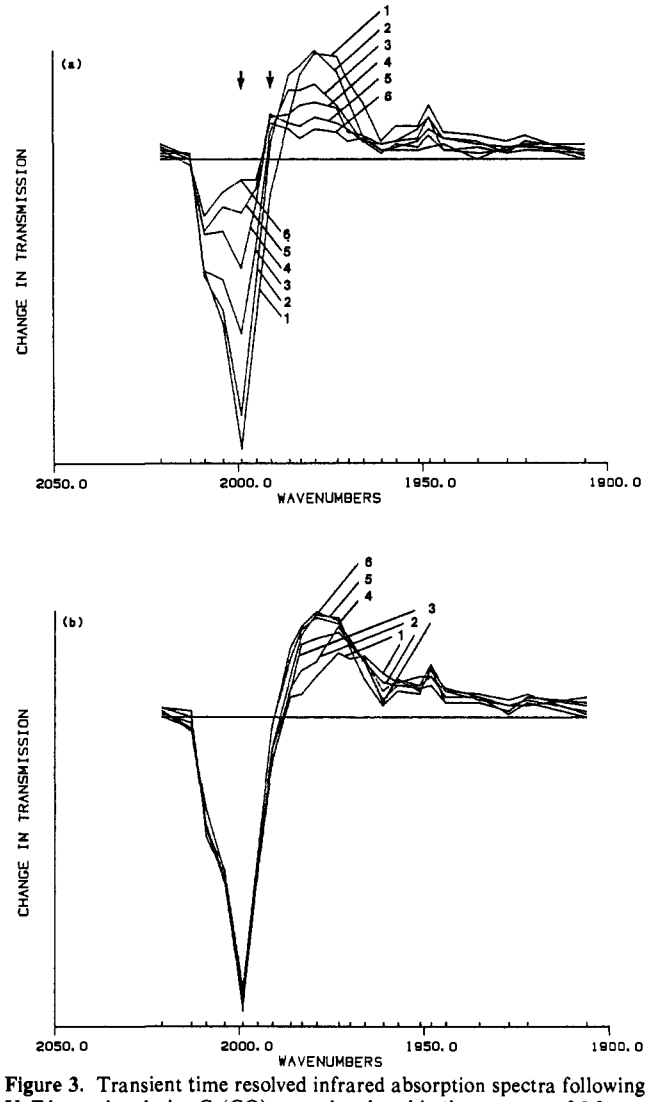

Figure 3. Transient time resolved infrared absorption spectra following XeF laser photolysis. $Cr(CO)_6$ was photolyzed in the presence of 5.0 torr of Ar and 0.3 Torr of CO in both cases. Spectrum a shows the evolution of the spectrum over a 2-μs range which has been segmented into 6 equal time intervals (labeled 1–6). The arrows denote the position of absorption bands of a polynuclear species (see text). Spectrum b shows the evolution of the spectrum over a 0.5-μs range which has been segmented into 6 equal time intervals. Note that the most prominent positive absorption shifts to higher freqeuncy as it grows into the spectrum.

3 effectively competes with reaction 2. Since the conditions were such that the concentration of CO was 10-fold greater than that of $Cr(CO)_6$, this indicates that the rate constant of reaction 3 must be *at least* as large as that of reaction 2. We note that the reported gas-phase rate constant of reaction 4, $3.4 \pm 0.5 \times 10^{14}$ cm^3 mol^{-1} s^{-1},[16] is $\sim$20-fold greater than that of reaction 2.

KrF Laser Photolysis. The transient spectrum 0.5 μs following KrF laser photolysis is shown in Figure 2b. The KrF laser supplies an input energy of 115 kcal/mol. Since the average Cr–CO bond energy of $Cr(CO)_6$ is 27 kcal/mol, formation of at least $Cr(CO)_3$, as well as $Cr(CO)_4$ and $Cr(CO)_5$, could be energetically possible. The KrF spectrum in Figure 2b shows, however, that only two broad bands dominate the spectrum. The band at $\sim$1920 cm^{-1} (labeled y) is assigned to the B_2 mode of C_{2v} $Cr(CO)_4$. Again, the B_1 and A_1 modes of $Cr(CO)_4$ are overlapped in the gas phase and comprise the band at $\sim$1957 cm^{-1} (labeled x) in Figure 2b. The remaining high-frequency A_1 vibration expected for C_{2v} $Cr(CO)_4$ is not observed, presumably because of its inherent weakness, and/or overlap with rovibrationally excited CO. That little of the pentacarbonyl is formed is evidenced by the very weak absorption in the region corresponding to the E mode of $Cr(CO)_5$.[14] Also note that in this case a weak absorption appears in the expected region ($\sim$2020 cm^{-1}) for $CO(v = 2)$.

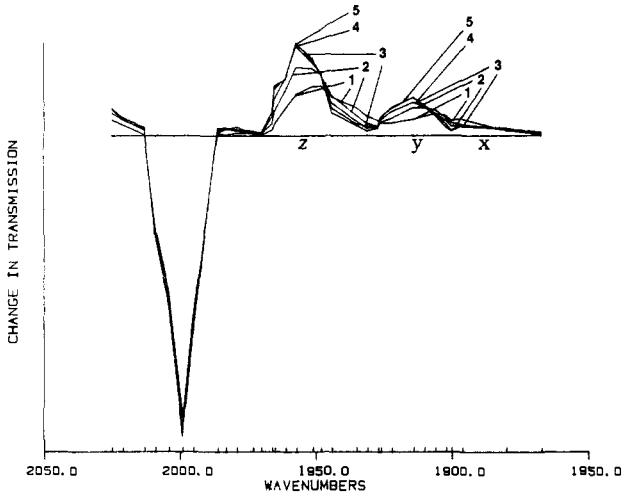

Figure 4. Transient time-resolved infrared absorption spectrum following KrF laser photolysis of $Cr(CO)_6$. The photolysis cell contained only $Cr(CO)_6$ and 5 Torr of Ar. The spectrum is displayed over a 1-μs range which is segmented into 5 (labeled) equal time intervals. Note that the very weak absorption below 1900 cm^{-1} (x) is intially overlapped with a more intense shifting absorption which shifts to higher frequency with time (y). The most intense positive absorption (z) is also observed to shift to higher frequency as it grows into the spectrum.

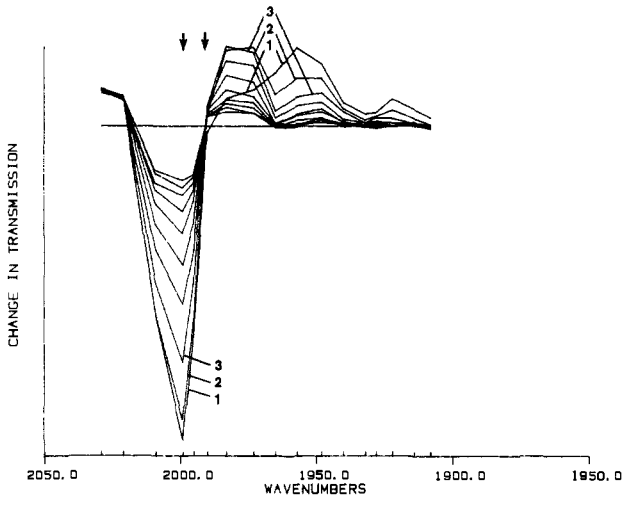

Figure 5. Transient time-resolved infrared absorption spectrum following KrF laser photolysis of $Cr(CO)_6$. Besides $Cr(CO)_6$, the photolysis cell contained 5.0 Torr of Ar and 0.5 Torr of CO. The spectrum is displayed over a 10-μs range which is segmented into 10 equal time intervals. The first 3 time intervals are labeled. The arrows denote absorptions of a polynuclear species (see text).

In an Ar matrix $Cr(CO)_3$ is postulated to adopt a C_{3v} structure, with an absorption at 1867 cm^{-1} (E) (Table I). From this information it is expected that in the gas phase C_{3v} $Cr(CO)_3$ would have an absorption around 1887 cm^{-1}. In this area only a very slight absorption, which is initially convoluted with the bands of vibrationally–rotationally excited $Cr(CO)_4$ (not bands) (vita infra), of $Cr(CO)_4$, is observed. Following relaxation of $Cr(CO)_4$, the intensity ratio of the remaining absorption at ~1880 cm^{-1} to the B_2 mode of $Cr(CO)_4$ is approximately 1 to 5. Relative yields of the products drawn from a comparison of the intensity ratio of the E mode of C_{3v} $Cr(CO)_3$ to the B_2 mode of $Cr(CO)_4$ on the basis of simple intensity arguments, which do not rigorously account for geometric and electrostatic coupling effects, are dubious. Nevertheless, we note that the ratio of KrF laser generated $Cr(CO)_4$ to $Cr(CO)_3$, measured via gas-phase chemical trapping, is also approximately 5 to 1.[11] Thus, for both results to be in agreement, the extinction coefficient of the two modes being compared must be roughly equal. This requirement is not unlikely to be met, and we concur with Tumas et al.[11] that $Cr(CO)_3$ is indeed formed via 248-nm photolysis of gas-phase $Cr(CO)_6$. This is contrary to the results reported by Fletcher and Rosenfeld.[16] These workers report that no infrared absorptions were observed in the 1890–1830-cm^{-1} region following 248-nm photolysis of gas-phase $Cr(CO)_6$. This may be due to lower signal-to-noise levels in their experiments. Further discussion of $Cr(CO)_3$ and its reaction with CO will be deferred until the distribution of products resulting for ArF photolysis is discussed.

Significant internal excitation of the nascent $Cr(CO)_4$ is possible since, taking the sum of the bond dissociation energies to be ~77 kcal/mol for loss of two CO's from $Cr(CO)_6$, ~38 kcal/mol are available for partitioning between internal and translational degrees of freedom of the products. As explained for the case of $Cr(CO)_5$, excitation of internal degrees of freedom manifests itself via a shift to higher energy of both the absorption features attributed to $Cr(CO)_4$ in the time-resolved spectrum of Figure 4. The spectra in this overlap plot are separated by successive 0.2-μs intervals. Notice that the bands assigned to $Cr(CO)_4$ (y and z) are initially significantly shifted to lower frequency than their final positions.

The absorption at 1880 cm^{-1} (x in Figure 4) is, as previously mentioned, that of C_{3v} $Cr(CO)_3$. Further convincing evidence that the two prominant features in Figure 4 do indeed represent $Cr(CO)_4$ can be demonstrated by promoting the reaction

$$Cr(CO)_4 + CO \xrightarrow{k_{45}} Cr(CO)_5 \qquad (5)$$

A time-resolved infrared spectrum of KrF laser photolyzed $Cr(CO)_6$ in the presence of 0.5 Torr of CO is shown in Figure 5. From this spectrum it is clear that as the bands attributed to C_{2v} $Cr(CO)_4$ disappear, the E mode of $Cr(CO)_5$ (1980 cm^{-1}) appears, and the formation of $Cr(CO)_6$ coincides with the disappearance of $Cr(CO)_5$. Over a range of added CO pressures of 0.5 to 4 Torr, the rate of disappearance of the $Cr(CO)_4$ absorption monitored at 1965 and 1914 cm^{-1} is, within experimental error, equal to the rate of appearance of the $Cr(CO)_5$ absorption mentioned at 1976 cm^{-1}. From Figure 6, which displays the pseudo-first-order decay rate of the $Cr(CO)_4$ absorptions plotted against the pressure of added CO, a second-order rate constant of $(2.0 \pm 0.3) \times 10^{13}$ cm^3 mol^{-1} s^{-1} can be deduced for reaction 5. This value is consistent with a previously reported value of k_{45}.[16a] Since the ground states of $Cr(CO)_4$ and $Cr(CO)_5$ are almost certainly singlets, reaction 5 is a spin-conserving process. This is yet another example of a coordinatively unsaturated species undergoing a spin-conserving reaction with near gas kinetic efficiency. Further studies are

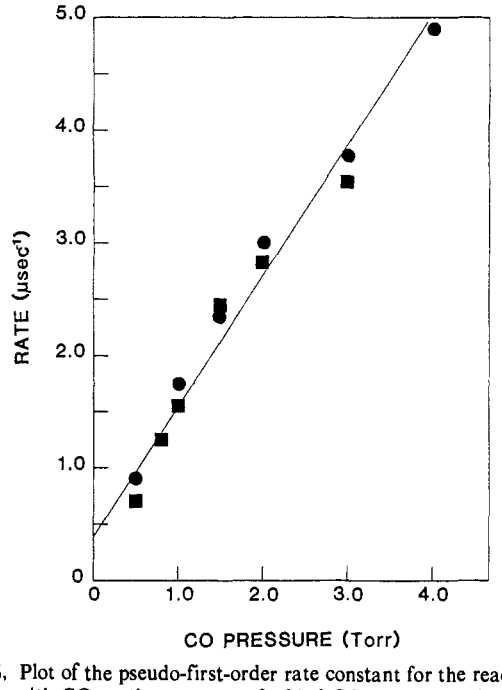

Figure 6. Plot of the pseudo-first-order rate constant for the reaction of $Cr(CO)_4$ with CO vs. the presence of added CO. The rate of $Cr(CO)_4$ disappearance was measured at 1965 cm^{-1} (■) and 1914 cm^{-1} (●). The slope of the curve gives a value of the bimolecular rate constant, k_4, of $(2.0 \pm 0.3) \times 10^{13}$ cm^3 mol^{-1} s^{-1}.

necessary to determine if this is a pervasive phenomenon.

Another important result is implicitly illustrated in Figure 6. Stabilization of the activated complex formed via collision of a CO molecule with $Cr(CO)_4$ requires the presence of a third body, i.e.,

$$Cr(CO)_4 + CO \xrightarrow{k_a} [Cr(CO)_4(CO)]^* \quad (6)$$

$$[Cr(CO)_4(CO)]^* \xrightarrow{k_r} Cr(CO)_4 + CO \quad (7)$$

$$[Cr(CO)_4(CO)]^* + M \xrightarrow{k_b} Cr(CO)_5 + M \quad (8)$$

The rate of $Cr(CO)_5$ formation is therefore, in principle, dependent upon the *total* pressure of the third body M. (If there is more than one species present which can stabilize the complex $[Cr(CO)_4(CO)]^*$ then k_b will be a weighted sum of k_M's.) However, our experimental conditions are such that the rate for reaction 8 is $\gg$ than the rate for reaction 7. This can be demonstrated by the independence of the rate constant for reaction of $Cr(CO)_x$ with CO on third-body pressure. The rate constant for reaction of $Cr(CO)_x$ with CO has been shown to be independent of rare gas buffer pressure between 5 and 15 Torr. In these experiments the rate constant for reaction was determined by variation of the CO pressure for different values of the rare gas buffer pressure over the previously stated range of rare gas pressures. In addition, the variation of the pseudo-first-order rate of reaction of $Cr(CO)_x$ with CO is observed to be linear in CO pressure. This latter independence of the rate constant for reaction of $Cr(CO)_x$ with CO on CO pressure is illustrated in Figure 6 and has also been reported by Fletcher and Rosenfeld for the reaction of $Cr(CO)_4$ + CO even *without* added rare-gas buffer.[16a] If the rate of reaction 8 was not $\gg$ than the rate of reaction 7, curvature in the plot of the rate of reaction of $Cr(CO)_4$ + CO would be expected. This has not been observed in our study or in the study of ref 16a. In addition, calculations of the expected lifetime of $[Cr(CO)_4CO]^*$ based on RRKM theory are compatible with these statements. However, recently Fletcher and Rosenfeld have reported observing a rare-gas buffer dependence on the rate constant for reaction of $Cr(CO)_4$ + CO.[16b] In their experiments the rate constant for reaction at a given CO and buffer gas pressure is deduced from a measurement of the rate of reaction at *one* CO pressure. These types of measurements are more susceptible to experimental artifacts and to kinetic processes that effect the intercept but not the slope of a rate vs. CO pressure plot. This may explain the discrepancy between the data reported here and those in ref 16b. Alternatively CO may be a much more efficient stabilizer of the activated complex than a rare gas.

It is evident, from Figure 5, that with KrF photolysis as with XeF photolysis, even in the presence of CO, reactions leading to the formation of polynuclear compounds occur. Evidence for this is the long-lived absorption at 1991 cm^{-1} (weak, but present) and the "flattening" of the T_{1u} band of the parent as it approaches the base line. We believe that this "flattening" effect is caused by an overlap of an absorption of a polynuclear species with the parent at 1999 cm^{-1}. These two subtle features are marked by arrows in Figure 5. The polynuclear species responsible for this distortion is most likely the same species responsible for the distortion of the parent band in Figure 3a which was tentatively identified as $Cr_2(CO)_{11}$. This could be formed by reaction of $Cr(CO)_5$ (either nascent or that produced via reaction 5) with $Cr(CO)_6$.

Since the distribution of fragments formed upon KrF laser photolysis is strongly dominated by $Cr(CO)_4$, the formation of $Cr_2(CO)_{10}$ via reaction 4 is also anticipated. Further, a related study has reported that reaction 4 proceeds at a near gas kinetic rate.[16] The $Cr(CO)_{10}$ product reportedly exhibits an absorption at $\sim$1980 cm^{-1} and has a lifetime of greater than 1 ms,[16] subsequent to KrF laser photolysis of $Cr(CO)_6$ in the absence of CO. In long time scale KrF laser generated spectra in the absence of CO (not shown), a long-lived absorption at $\sim$1928 cm^{-1} is observed, as well as one at $\sim$1980 cm^{-1}. Upon addition of significant amounts of CO, the intensity of these absorptions decreases. Since nonphotolytic depletion and incomplete recovery of $Cr(CO)_6$ are observed, reaction 4 must compete with a fast reaction of $Cr(CO)_4$ with CO in the presence of a large excess of CO. Thus we concur that reaction 4 proceeds at a rate approaching gas kinetic.

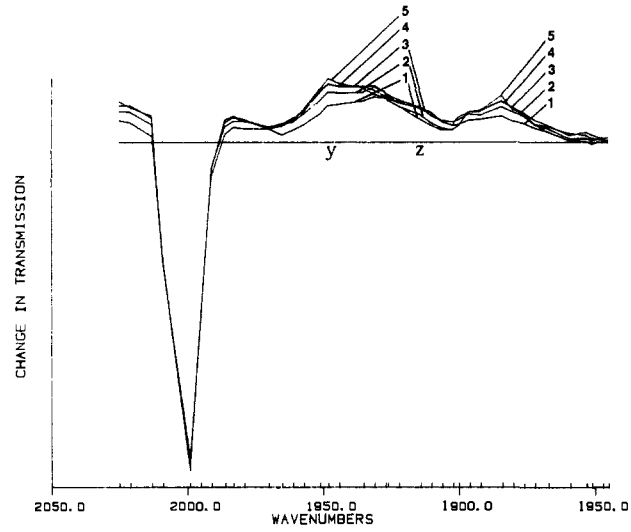

Figure 7. Transient time-resolved infrared absorption spectrum following ArF laser photolysis. Besides $Cr(CO)_6$, the photolysis cell contained 5.0 Torr of Ar. The spectrum is displayed over a 1.0-μs range which is segmented into 5 (labeled) equal time intervals.

ArF Laser Photolysis. The infrared spectrum 0.5 μs following ArF laser photolysis is shown in Figure 2c. The ArF laser inputs 149 kcal/mol. From the average energy of the Cr–CO bond, all of the $Cr(CO)_x$ fragments, where x = 5–1, could be formed upon ArF laser photolysis. Figure 2c shows that the infrared absorptions of some of these species, if not all, are overlapped, forming a broad, diffuse spectrum. It may, at first glance, appear that the distribution of photofragments generated upon ArF laser photolysis contains a higher percentage of $Cr(CO)_5$ molecules than that generated upon KrF laser photolysis, since the ArF laser generated spectrum shows a relatively more intense absorption at $\sim$1985 cm^{-1}. Note, however, that the absorptions at 2020 and $\sim$1985 cm^{-1} are both more intense in the ArF spectrum than they are in the KrF spectrum. While the 1985-cm^{-1} band in both spectra may partially represent nascent $Cr(CO)_5$, we believe that the majority of the intensity for the ArF spectrum is due to vibrationally hot (v = 3), photoejected CO. Absorption by vibrationally hot CO rationalizes the apparent formation of greater amounts of $Cr(CO)_5$ with ArF than with KrF photolysis. Mainly kinetic evidence is relied on to "sort out" the remainder of the spectrum.

The time-resolved ArF spectrum displayed in Figure 7 clearly shows that the broad band extending from $\sim$1965 to 1900 cm^{-1} is comprised of at least two different species since the higher frequency portion of the band ($\sim$1950 cm^{-1}, denoted as "y") is observed to grow in on a different time scale than the lower frequency portion ($\sim$1920 cm^{-1}, denoted as "z"). Whether the species absorbing at $\sim$1950 cm^{-1} grows in via reaction or vibrational relaxation is uncertain due to the overlap with the species absorbing at the lower frequency portion of this broad feature. Note, however, that C_{2v} $Cr(CO)_4$ absorbs at 1957 cm^{-1}. Since the bands of the KrF laser produced $Cr(CO)_4$ exhibits a shift to higher frequencies, which is indicative of internal excitation, and the input energy of the ArF laser is greater, it would be expected that ArF produced species would be significantly vibrationally/rotationally excited. Thus the bands of ArF laser generated $Cr(CO)_4$ are also expected to exhibit a shift to high frequency. The absorption band centered around 1880 cm^{-1} grows in on yet a different time scale and it is most likely due to the absorption of the probe beam by a single species. The reaction of these species with CO is the most effective method to ascertain their identity.

The time-resolved ArF spectrum of $Cr(CO)_6$ in the presence of 1 Torr of added CO is shown in Figure 8a. From this spectrum it is observed that the band centered at 1880 cm^{-1} and the 1930-cm^{-1} portion of the broad band rapidly disappear, while the

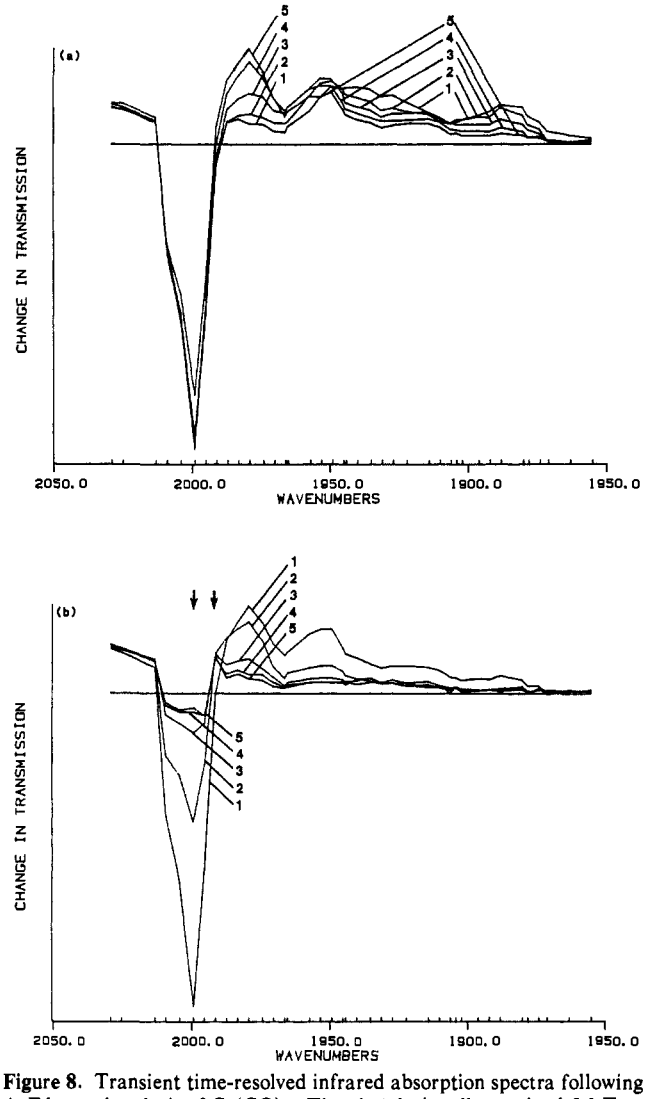

Figure 8. Transient time-resolved infrared absorption spectra following ArF laser photolysis of $Cr(CO)_6$. The photolysis cell contained 5.0 Torr of Ar and 1.0 Torr of CO as well as $Cr(CO)_6$. Spectrum a is displayed over a 2-μs range which is segmented into 5 (labeled) equal time intervals. Spectrum b is displayed over a 8-μs range which is segmented into 5 equal time intervals. The presence of polynuclear absorptions is indicated by arrows.

1957-cm^{-1} region of the broad band and a band corresponding to the E mode of $Cr(CO)_5$ grow in. There is also partial recovery of the parent. The absorption at 1957 cm^{-1} is certainly the B_1 and A_1 modes of C_{2v} $Cr(CO)_4$. The B_2 band of this species, centered around 1925 cm^{-1}, is obscured in this figure by overlapping absorptions. Clearly, the reaction of lower fragments with CO to form $Cr(CO)_4$ is being observed, which in turn reacts to form $Cr(CO)_5$ and ultimately parent (neglecting fragment–fragment and polynuclear-forming reactions). Identification of the lower fragments is easily performed by probing the 1880- and 1930-cm^{-1} region of the spectrum at various pressures of added CO. As mentioned earlier, C_{3v} $Cr(CO)_3$ is expected to absorb at ~1880 cm^{-1}. The rate constant for the species absorbing at 1880 cm^{-1}, measured from plots of the rate of the single exponential decay of the band against added CO pressure, is 1.8×10^{13} cm^3 mol^{-1} s^{-1}. Although in this spectrum it is not possible to accurately measure rise rates of the bands attributed to $Cr(CO)_4$ due to overlapping absorptions, the band at 1880 cm^{-1} is nevertheless assigned to C_{3v} $Cr(CO)_3$. Further note that the rise rate of the 1880-cm^{-1} band increases with CO pressure. Since this rate increase cannot be attributed to relaxation effects affected via the increase in total pressure upon CO addition (no "blue" shifting of the absorption band is observed), it is concluded that $Cr(CO)_2$ is also formed upon ArF photolyis. The reaction of nascent $Cr(CO)_2$ with CO to produce $Cr(CO)_3$ is the process

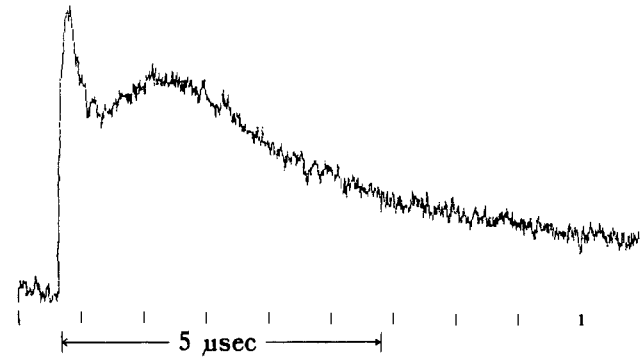

Figure 9. Temporal behavior of the 1914 cm^{-1} transient absorption in the presence of 0.5 Torr of CO. The absorption is attributed to two species (see text).

responsible for the above noted increase in the rise rate of the 1880-cm^{-1} band upon CO addition.

As noted earlier, the absorption at 1930 cm^{-1} is attributed to multiple species, and a probe of this band as a function of CO pressure is quite revealing. From Figure 9, which displays the temporal behavior of the transient absorption at 1914 cm^{-1}, it is clear that the fall rate of the species which grows in at a detector-limited rate is convoluted with the rise rate of another species. The absorption growing in on the longer time scale is undoubtedly attributed to the B_2 vibrational mode of C_{2v} $Cr(CO)_4$. Since $Cr(CO)_4$ can be generated via reaction of the more highly unsaturated fragment with CO, as the pressure of added CO is increased the intensity of the absorption growing in on a longer time scale is maximized at an earlier time relative to the photolysis pulse. Although the fall rate of the species responsible for the faster time scale absorption cannot be accurately measured and compared to the rise rate of the band assigned to $Cr(CO)_3$, the absorption having the detector limited rise at ~1914 cm^{-1} is attributed to $Cr(CO)_2$. It should be noted that in a CH_4 matrix a band observed at 1903 cm^{-1} was tentatively assigned to $Cr(CO)_2$.[5] The reason for the absorption of $Cr(CO)_2$ occurring at an unexpectedly high frequency in the matrix is not known. However, the difference in the frequencies in the gas phase and matrix is compatible with typical spectral shifts for these phases.

The absorptions at 1999 and 1995 cm^{-1} which have been previously attributed to Cr_2CO_{11} also appear in the transient time-resolved infrared absorption spectrum generated via ArF laser photolysis of chromium hexacarbonyl in the presence of added CO. The spectrum displayed in Figure 8b shows the evolution of the system over an 8-μs range. The frequency of the bands of the polynuclear species is marked by arrows in this figure. As was observed to occur upon XeF laser photolysis, the 1999-cm^{-1} band is overlapped with the $T_{1\mu}$ band of the parent molecule, distorting the latter. The polynuclear species is most likely formed via

$$Cr(CO)_5 + Cr(CO)_6 \rightarrow Cr_2(CO)_{11}$$

The $Cr(CO)_5$ fragment undoubtedly is produced through reaction of the more highly unsaturated species with CO.

IV. Conclusions

This study provides direct spectroscopic evidence for the production of $Cr(CO)_x$ (x = 5, 4, 3, 2) fragments in the gas phase following excimer laser photolysis of $Cr(CO)_6$. The absorption bands observed for all coordinatively unsaturated photofragments are compatible with the geometries deduced for these species in the condensed phase. This strongly implies that solid-state and solvent effects *do not* perturb the "ideal" gas-phase structure of these species. The identity of the photofragments produced upon gas-phase photolysis is, however, very different than those produced in the condensed phase. Absorption of a single UV photon in the gas phase can lead to ejection of more than one CO. In the condensed phase, fragments more coordinatively unsaturated than $Cr(CO)_5$ have only been reported via sequential photolysis of the primary coordinatively unsaturated species; only one CO is lost

Table II. Summary of the Bimolecular Rate Constants for $M(CO)_x$–CO Reactions

	spin allowed	rate constant (10^{-13} cm^3 mol^{-1} s^{-1})
$Cr(CO)_5 + CO \rightarrow Cr(CO)_6$	Y	1.5,[a,e] 2.2,[b] 0.4[c]
$Cr(CO)_4 + CO \rightarrow Cr(CO)_5$	Y	2.4,[a,e] 2.6[b]
$Cr(CO)_3 + CO \rightarrow Cr(CO)_4$	Y	1.8[e]
$Fe(CO)_4 + CO \rightarrow Fe(CO)_5$	N	0.003[d]
$Fe(CO)_3 + CO \rightarrow Fe(CO)_4$	Y	1.2[d]
$Fe(CO)_2 + CO \rightarrow Fe(CO)_3$	?	1.7[d]

[a] Reference 14. [b] Reference 16. [c] References 6 and 7. [d] References 13 and 22. [e] This work.

per absorption event. The differences between the gas and condensed phases can easily be rationalized if the primary photochemical event is loss of one CO in both phases. In the condensed phase the primary photofragment which is produced with significant internal vibration–rotation energy is rapidly relaxed (on a ps time scale) by collisions with the surrounding solvent or solid lattice *before* ejection of additional CO's can occur.

In the gas phase, at low pressure, internal vibration–rotation relaxation does not occur on a picosecond time scale. Supporting this is our observation of relaxation on a μs time scale at a total pressure of a few Torr. For μs relaxation times it would be expected that RRKM type dissociation of vibrationally energized molecules will compete effectively with relaxation of the primary photofragment leading to further photofragmentation. This mechanism would predict a monotonic increase in the degree of fragmentation as a function of increasing photolysis photon energy. It might be expected that a change in the character of the electronic state that is accessed as a function of photolysis wavelength would have an effect on the nature of the photoproducts, particularly in systems such as $Mn_2(CO)_{10}$ with two very different types of bonds. Whether the nature of the electronic state accessed also has a significant effect on the degree of fragmentation in $Cr(CO)_6$ will ultimately be answered by detailed wavelength dependent studies of fragmentation following UV photolysis. However, our results are at least qualitatively compatible with the primary photochemical event leading to loss of one CO followed by RRKM type dissociation of this product to produce greater fragmentation as the energy of the input photon and correspondingly the degree of internal vibration/rotation excitation of the primary photoproduct increases.

Kinetic information on the rates and pathways for reaction of the $Cr(CO)_x$ fragments has also been obtained. Table II provides a summary of the rates of reaction of $Cr(CO)_x$ species with CO. For comparison the rates of reaction of $Fe(CO)_x$ species with CO are also displayed. Interestingly, the only reaction that is not of the same order as all the others is the reaction of $Fe(CO)_4 + CO$. This reaction is known to be a spin-disallowed reaction going from triplet $Fe(CO)_4$ to singlet $Fe(CO)_5$. All the other reactions are much faster, approximately an order of magnitude less than expected for a gas kinetic reaction cross section. An inference of the similar, rapid increases of these species is that all other reactions in Table I and thus all the reactions in the $Cr(CO)_x$ system are spin allowed.

Finally, in accord with the high reactivity of the $Cr(CO)_x$ fragments, $Cr(CO)_4$ and $Cr(CO)_5$ have both been observed to rapidly react with parent to form polynuclear organometallic compounds. The observation of reactions of these species with parent is in accord with the results of previous studies.[10,16] In addition, we report the position of some of the gas-phase absorptions of the polynuclear species which are tentatively assigned to $Cr_2(CO)_{10}$ and $Cr_2(CO)_{11}$, formed via reaction of $Cr(CO)_4$ and $Cr(CO)_5$ with parent.

Acknowledgment. We thank the Air Force Office of Scientific Research for support of this work under Contract 83-0372. We also acknowledge support of this work by the donors of the Petroleum Research Fund, administered by the American Chemical Society. We thank Dr. Martyn Poliakoff for some very useful and informative discussions and are grateful for support from NATO which facilitated these discussions. We also thank Prof. Robert Rosenfeld for providing us with access to his data prior to publication.

Registry No. $Cr(CO)_6$, 13007-92-6; $Cr(CO)_5$, 26319-33-5; $Cr(CO)_4$, 56110-59-9; $Cr(CO)_3$, 81714-33-2; $Cr(CO)_2$, 102869-00-1; CO, 630-08-0.